NANOSYSTEMS: PHYSICS, CHEMISTRY, MATHEMATICS, 2021, 12 (3), P. 283–290

Prooxidant potential of CeO_2 nanoparticles towards hydrogen peroxide

M. M. Sozarukova[1], E. V. Proskurnina[2], V. K. Ivanov[1]

[1]Kurnakov Institute of General and Inorganic Chemistry, Russian Academy of Sciences, Leninsky Prospect, 31, Moscow, 119991, Russia

[2]Research Centre for Medical Genetics, Moskvorechie St, 1, Moscow, 115522, Russia

s_madinam@bk.ru, proskurnina@gmail.com, van@igic.ras.ru

PACS 68.65.k, 81.20.n, 82.70.Dd, 87.85.Rs **DOI 10.17586/2220-8054-2021-12-3-283-290**

The multifaceted enzyme-like activity of CeO_2 nanoparticles (CeNPs) expands the prospects for their potential biomedical applications. In this regard, there is a need for a comprehensive analysis of the redox behavior of CeO_2 nanoparticles in relation to key molecules of free radical homeostasis. Here, the prooxidant potential of CeNPs towards H_2O_2 was investigated to elucidate both prooxidant capacity and prooxidant activity of CeNPs. To describe the kinetics in the luminol–H_2O_2 system at pH 8.5 upon the addition of citrate-stabilized CeO_2 sol (3 nm), a numerical model of three reactions is proposed. The rate constants being a measure of prooxidant activity, were $k_1 = 9.0 \cdot 10^4$ $\mu M^{-1}min^{-1}$, $k_2 = 2.0 \cdot 10^{-6}$ $\mu M^{-1}min^{-1}$, $k_3 = 2.9 \cdot 10^{-5}$ $\mu M^{-1}min^{-1}$. The functionalization of CeO_2 nanoparticles surface with ammonium citrate increases their prooxidant capacity by two-fold, while modification with maltodextrin decreases it by six-fold. It was shown that the prooxidant capacity of citrate-stabilized CeO_2 sol in Tris-HCl is approximately four-fold higher than in phosphate buffer solution at pH 7.4.

Keywords: cerium dioxide nanoparticles, nanozymes, hydrogen peroxide, luminol, peroxidase, chemiluminescence, prooxidant, ammonium citrate, maltodextrin, mathematical modeling.

Received: 13 May 2021

1. Introduction

Cerium dioxide nanoparticles have a wide spectrum of nanozyme (enzyme-like) activities [1–6]. The ability to mimic the functions of a number of enzymes is due to the unique physicochemical properties of CeO_2 nanoparticles. The combination of the pro- and antioxidant properties of nanodisperse CeO_2 with its relatively low toxicity expands the field of its potential biomedical applications [7–11]. In turn, this makes it necessary to study the redox behavior of CeO_2 nanoparticles in relation to the key molecules of free radical homeostasis.

Among the types of enzyme-like activity of nanodisperse CeO_2, their functioning as peroxidase mimetics is important. Hydrogen peroxide is the most abundant reactive oxygen species and is involved in free radical metabolism [12]. Dismutation of superoxide anion radicals (SAR) catalyzed by superoxide dismutase (SOD) in biological tissues inevitably leads to the formation of H_2O_2 molecules that easily penetrate cell membranes. On the other hand, cerium dioxide nanoparticles exhibit SOD-like activity and, accordingly, the formation of hydrogen peroxide takes place when cerium dioxide acts as a SOD mimetic [1, 13, 14]. Thus, the study of the redox behavior of CeO_2 nanoparticles towards to hydrogen peroxide needs to be considered when analyzing SOD-like ceria activity. Currently, increasing attention is being paid not only to the cytotoxic function of H_2O_2 found in phagocytosis, mitochondrial and microsomal function, but also to its involvement in the regulation of cell signaling and transcription factors [15, 16]. Hydrogen peroxide plays an important role in cell proliferation [17], differentiation [18], migration [19] and apoptosis [20].

In this work, we analyzed the prooxidant potential of nanodisperse CeO_2 towards hydrogen peroxide according to the data of chemiluminescence analysis. Here, we consider prooxidant potential as a complex characteristic, combining both the prooxidant capacity (the number of formed reactive oxygen species per unit concentration of the prooxidant) and the prooxidant activity (the rate constant of the total reaction of the production of reactive oxygen species).

2. Materials and methods

2.1. Synthesis and physicochemical study of CeO_2 nanoparticles

An unstabilized aqueous colloidal solution of cerium dioxide nanoparticles (0.13 M) was prepared by thermohydrolysis of ammonium cerium(IV) nitrate (#215473, Sigma-Aldrich) [21]. Briefly, an aqueous solution of ammonium cerium(IV) nitrate (100 g/l) was kept for 24 h in an oven at 95°. The precipitate formed was separated by centrifugation and washed three times with isopropanol. To completely remove isopropanol, the resulting precipitate was redispersed in deionized water, followed by boiling for 1 h with constant stirring. The concentration of CeO_2 sol was determined

by the thermogravimetric method. Thus prepared colloidal solution of CeO_2 nanoparticles was stabilized with ammonium citrate ($C_6H_{14}O_7N_2$, disubstituted ammonium citrate, #247561, Sigma-Aldrich) or maltodextrin (#419672, dextrose equivalent 4.0–7.0, Sigma-Aldrich) in a molar ratio of 1 : 1 and 1 : 1.1, respectively.

X-ray diffraction patterns of nanodisperse CeO_2 samples were obtained using a Bruker D8 Advance diffractometer (Cu$K\alpha$ radiation, geometry θ–2θ). The diffraction maxima were identified using the ICDD PDF2 database. The average hydrodynamic diameter of CeO_2 nanoparticles was estimated by dynamic light scattering using a Photocor Complex analyzer. The microstructure of the samples was studied by transmission electron microscopy on a Leo 912 AB Omega electron microscope at an accelerating voltage of 100 kV. UV-visible absorption spectra of CeO_2 sols were recorded using on OKB Spectr SF-2000 spectrophotometer.

3. The study of prooxidant activity in the chemiluminescent system luminol – H_2O_2

Luminol (5-amino-1, 2, 3, 4-tetrahydro-1, 4-pthalazinedione, 3-aminophthalic acid hydrazide, #A8511, Sigma-Aldrich) was used as a chemiluminescent probe (CL probe) sensitive to H_2O_2. A working solution with a concentration of 1 μM was prepared by dissolving a weighed amount of a CL probe in a 100 μM phosphate buffer solution (PBS, KH_2PO_4, #60220, Sigma-Aldrich), with further addition of KOH (#484016, Sigma-Aldrich) until the luminol was completely dissolved. After that, pH of the solution was adjusted to 7.4 using concentrated HCl (#320331, Sigma-Aldrich). Working solutions of hydrogen peroxide were prepared by diluting a stock solution of H_2O_2 (30%, #8.22287, Sigma-Aldrich). We also used a 100 μM buffer solution (pH 7.4) prepared from Tris hydrochloride (#10812846001, Merck).

Chemiluminescence (CL) was recorded on a 12-channel Lum-1200 chemiluminometer (DISoft) at room temperature. Aliquots of luminol (50 μM) and hydrogen peroxide (200 μM) were added to a plastic cuvette containing PBS. The analyzed sample was added to the luminol–H_2O_2 system 30–60 s after the start of the background emission recording. The total volume of the system was 1.000 ml. The light sum (area under the chemiluminescence curve) for 5 min was chosen as an analytical signal.

Mathematical simulation of chemiluminograms was carried out using the Kinetic Analyzer software (developed by D. Yu. Izmailov). As a result, the rate constants of the interaction of CeO_2 nanoparticles with the reaction substrate, which are a measure of prooxidant activity, were determined.

4. Results and discussion

Thermolysis of aqueous solution of ammonium cerium(IV) nitrate resulted in formation of electrostatically stabilized sol of nanodisperse cerium dioxide. The concentration of the CeO_2 sol, determined by the thermogravimetric method, was 23 g/l (0.13 M). The results of X-ray diffraction analysis indicated that the resulting sol contained single-phase cerium dioxide (PDF2 34-0394). The size of the obtained CeO_2 nanoparticles determined by Scherrer equation was found to be 3 nm. The data on the particle size and phase composition of the obtained CeO_2 samples were confirmed by transmission electron microscopy and electron diffraction.

According to the dynamic light scattering data, the average hydrodynamic diameters of CeO_2 nanoparticles without a stabilizer and those modified with ammonium citrate or maltodextrin were 11–12 nm, 16 nm and 17 nm, respectively. Insignificant changes in the hydrodynamic diameter upon interaction with stabilizers indicate approximately the same degree of particle aggregation in CeO_2 sols. The absorption spectra of the analyzed samples are shown in Fig. 1, the appearance of an absorption band in the region of 280–300 nm confirms the fact that the sols do contain nanodispersed cerium dioxide.

It is generally believed that the redox behavior of CeO_2 nanoparticles is determined by many factors, among which the pH of the reaction medium plays an important role. The effect of pH (4.0, 7.4, 8.5) on chemiluminescence in the luminol–H_2O_2 system was investigated upon the addition of nanodisperse cerium dioxide (Fig. 2).

For non-stabilized colloidal solution of cerium dioxide nanoparticles, as well as for the colloidal solution of CeO_2 nanoparticles stabilized with ammonium citrate, the highest CL response in the system was observed at pH 8.5. According to the existing data, a decrease in pH enhances the oxidative properties of Ce^{4+} ions [22]. A pronounced peroxidase-like activity of CeO_2 nanoparticles was reported at pH 4.0 [22]. In our study, neither the addition of CeO_2 nanoparticles nor the addition of Fe^{2+} ions to the system (hemoglobin solution, data not shown) caused any changes at this pH value. The mechanism of chemiluminescence during luminol oxidation in an aqueous solution has been extensively studied [23–25]. Hydroxyl and superoxide anion radicals are important intermediate products contributing to luminescence [23,24]. Since both $\cdot O_2^-$ and the luminol hydroperoxide anion participating in the luminol chain of transformations are stable in an alkaline medium only, the quantum yield of luminol-dependent CL increases dramatically with increasing pH [26]. In neutral and acidic media, the contribution of side reactions not accompanied by chemiluminescence seems to prevail [27].

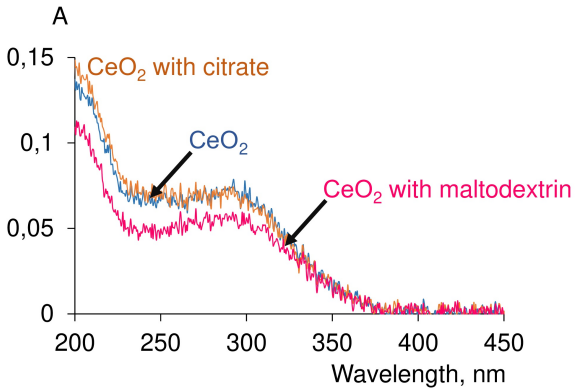

FIG. 1. Absorption spectra of CeO_2 sols (non-stabilized, citrate-stabilized and maltodextrin-stabilized)

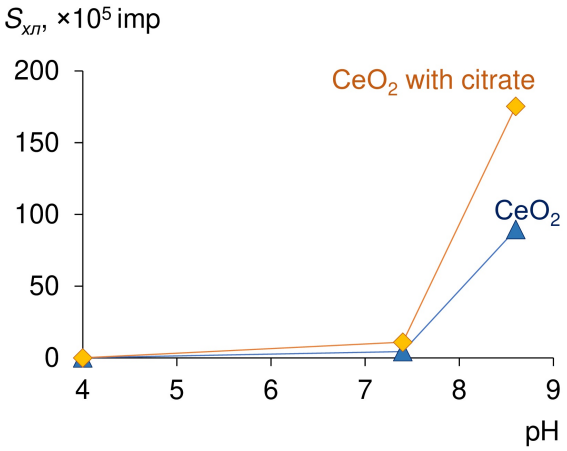

FIG. 2. Dependences of the CL light sum (S_{CL}, $\times$ 10^5 imp) on pH (4.0; 7.4; 8.5) upon the addition of CeO_2 sols (both non-stabilized and citrate-stabilized) to the luminol–H_2O_2 system in 100 μM PBS. Conditions: 50 μM luminol, 500 μM H_2O_2, 1.0 μM CeO_2 sol

At pH 8.5 kinetic curves were recorded in the luminol–H_2O_2 system depending on the concentrations of both the citrate-stabilized CeO_2 sol (Fig. 3a) and the H_2O_2 substrate (Fig. 3c).

CL intensity increased with increasing concentration of citrate-stabilized CeO_2 sol added to the system (Fig. 3a) and hydrogen peroxide (Fig. 3c). Thus, CeO_2 nanoparticles in the luminol–H_2O_2 system exhibited prooxidant activity. As an analytical signal, we chose the CL light sum (S_{CL}, the area under the CL curve for 5 min), proportional to the concentration of free radicals formed in the system, which can serve as a measure of the prooxidant capacity of the analyzed sample. Fig. 3b,d show the dependences of the analytical signal on the concentration of citrate-stabilized CeO_2 sol and H_2O_2, respectively. In the absence of a catalyst, the reaction of luminol with H_2O_2 in alkaline medium proceeds relatively slowly and is characterized by weak CL.

Nanodispersed cerium dioxide exhibits multifaceted activity towards hydrogen peroxide [14]. At pH $>$ 6.0, the peroxidase-like properties of nanodisperse CeO_2 are absent, since at high pH values CeO_2 nanoparticles act as catalase [22]. However, stoichiometric CeO_2 nanoparticles obtained by high-temperature treatment can exhibit peroxidase-like properties even at higher pH [28]. For example, at pH 7.2, due to the peroxidase-like activity, they accelerated the interaction of H_2O_2 with luminol and enhanced the luminescence of the latter [28]. Our data demonstrate the prooxidant function of citrate-stabilized CeO_2 sol towards H_2O_2 in the presence of luminol at pH $>$ 6. The addition of CeO_2 nanoparticles leads to the high luminescence intensity with exponential type decay. Comparison of chemiluminograms of nanodispersed cerium dioxide and horseradish peroxidase showed a smooth increase in the luminescence intensity with a subsequent stationary luminescence level, confirming different mechanisms of processes occurring in these systems [29]. Thus, an assumption can be drawn that, in the luminol–H_2O_2 system, ceria nanoparticles act by a nonenzymatic mechanism. To support this assumption, the method of mathematical modeling was used

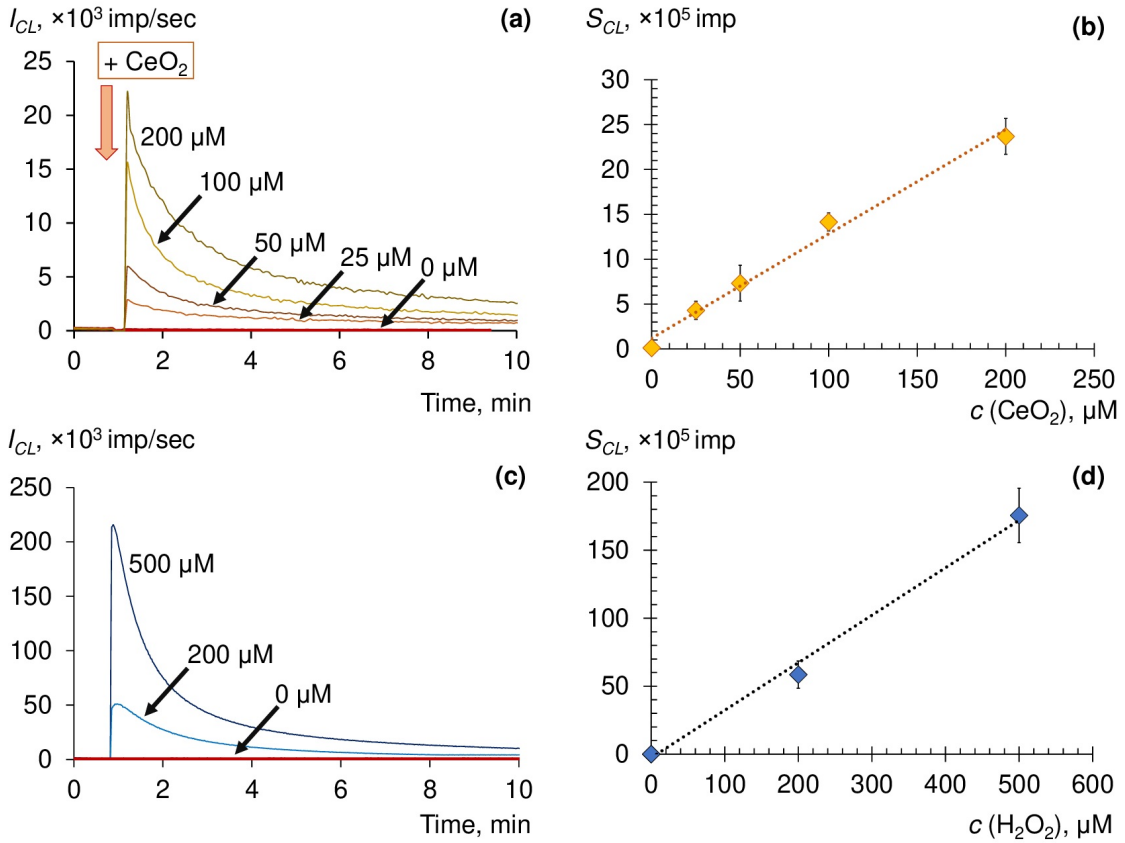

FIG. 3. Chemiluminograms for the luminol–H_2O_2 system in 100 μM PBS (pH 8.5) (a) with the addition of citrate-stabilized CeO_2 sol, (c) containing different concentrations of H_2O_2 with the addition of citrate-stabilized CeO_2 sol. The dependence of the light sum (S_{CL}, $\times$ 10^5 imp) on the concentration of (b) citrate-stabilized CeO_2 sol, (d) H_2O_2. Conditions: (a) 50 μM luminol, 200 μM H_2O_2, citrate-stabilized CeO_2 sol (concentrations are shown in the Figure), (b) 50 μM luminol, H_2O_2 (concentrations are shown in the Figure), 1 μM citrate-stabilized CeO_2 sol

our approach was based on developing a mathematical model of a system of chemical reactions and calculating their rate constants.

Studies of the peroxidase-like activity of nanodisperse cerium dioxide have previously shown that its action is similar to the mechanism of catalysis by other nanoparticles [30–34]. Constants were selected for reactions (1)–(6), which, according to the literature, describe the most probable mechanism of the redox behavior of CeO_2 nanoparticles towards H_2O_2 in the presence of luminol [22, 31, 33]:

$$H_2O_2 + OH^- \rightarrow HO_2^- + H_2O, \quad k_1 = 9.4 \cdot 10^{-14}\ \mu M^{-1}min^{-1}, \tag{1}$$

$$Lum + OH^- \rightarrow Lum^- + H_2O, \quad k_2 = 1.9 \cdot 10^{-15} \mu M^{-1}min^{-1}, \tag{2}$$

$$H_2O_2 + CeNPs \rightarrow 2OH\cdot, \quad k_3 = 7.9\ \mu M^{-1}min^{-1}, \tag{3}$$

$$OH\cdot + HO_2^- \rightarrow O_2^- + H^+, \quad k_4 = 6.4 \cdot 10^{10} \quad \mu M^{-1}min^{-1}, \tag{4}$$

$$OH\cdot + Lum^- \rightarrow \cdot Lum^-, \quad k_5 = 2.4 \cdot 10^{-8} \quad \mu M^{-1}min^{-1}, \tag{5}$$

$$\cdot O_2^- + \cdot Lum^- \rightarrow 3APA*, \quad k_6 = 6.0 \cdot 10^{-15} \quad \mu M^{-1}min^{-1}, \tag{6}$$

$$3APA* \rightarrow 3APA + h\nu, \quad k_7 = 9.9 \cdot 10^{-1} \quad \mu M^{-1}min^{-1}, \tag{7}$$

where Lum, Lum^- and $\cdot Lum^-$, 3APA$*$ refer to luminol, luminol anion, luminol radical and 3-aminophthalate anion, respectively.

Kinetic modeling of experimental data is shown in Fig. 4.

Kinetic behavior is similar to the chemiluminescence curves obtained for horseradish peroxidase [29], and significantly differs from the experimental data for CeO_2 sols obtained in the present study. The formation of 3-aminophthalate anions, hydroxyl and superoxide anion radicals plays a key role in the enhancement of CL induced

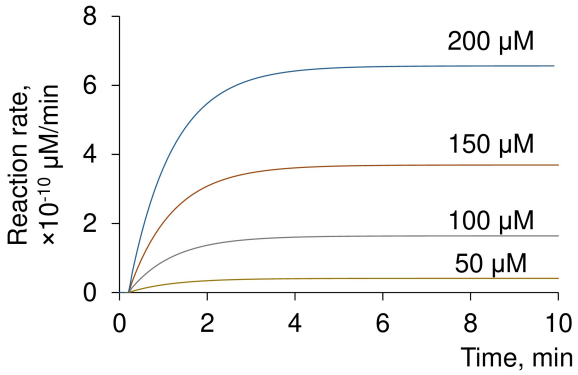

FIG. 4. Kinetic modeling of experimental data in the CL system luminol–H_2O_2 with CeO_2 nanoparticles. Conditions: 50 μM luminol, 200 μM H_2O_2, CeO_2 sol (concentrations are shown in the figure)

by the addition of CeO_2 nanoparticles as confirmed by analysis of absorption spectra (425 nm — absorption band of 3-aminophthalate) and inhibitory analysis using SOD (for enzymatic dismutation of SAR) and selective traps for hydroxyl radicals — *tert*-butanol, *n*-butanol, and mannitol [31]. Possible participation of oxygen dissolved in the reaction medium in the interaction with luminol and SAR radicals should be taken into account as demonstrated earlier in the experiments on deaeration with CuO nanoparticles [35]. In the same study, it was found that the enhancement factor of nanoparticles on luminol–H_2O_2 CL system for CuO is 400 [35], while for CeO_2 nanoparticles it is 22.5 [31].

We proposed the following simplified model as a possible mechanism for the prooxidant activity of CeO_2 nanoparticles towards H_2O_2:

$$\text{CeNPs} + H_2O_2 \rightarrow 2\text{OH}\cdot, \quad k_1 = 9.0 \cdot 10^4\ \mu\text{M}^{-1}\text{min}^{-1}, \tag{8}$$

$$\text{Lum} + \text{OH}\cdot \rightarrow \text{Lum}*, \quad k_2 = 2.0 \cdot 10^{-6}\ \mu\text{M}^{-1}\text{min}^{-1}, \tag{9}$$

$$\text{Lum}* + \text{Lum}* \rightarrow \text{P} + \text{h}\nu, \quad k_3 = 2.9 \cdot 10^{-5}\mu\text{M}^{-1}\text{min}^{-1}, \tag{10}$$

where Lum$*$ is luminol in an excited state, P is the CL reaction product.

For the given initial concentrations of the reactants the reaction rate constants were selected. Comparison of the experimental data for citrate-stabilized CeO_2 sol and fitting results is shown in Fig. 5.

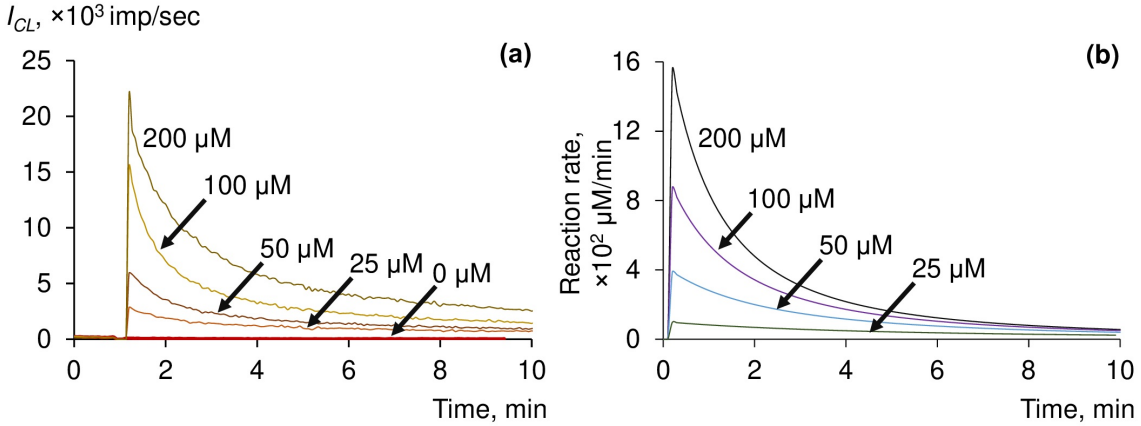

FIG. 5. Chemiluminescence of the luminol–H_2O_2 system in 100 μM PBS (pH 8.5) upon the addition of the citrate-stabilized CeO_2 sol (a), fitting of the experimental data (b). Conditions: 50 μM luminol, 200 μM H_2O_2, CeO_2 sol (concentrations are shown in the figure)

The proposed basic model agrees well with the experimental data. The rate constants of interaction of CeO_2 nanoparticles with the reaction substrate can be judged as a measure of their prooxidant activity.

The formation of highly reactive hydroxyl radicals in the presence of CeO_2 nanoparticles was confirmed and studied by various methods [36–38]. Some researchers associate the catalytic activity of CeO_2 nanoparticles with the formation of peroxide-like intermediates [39, 40]. Despite various assumptions regarding the mechanism of ceria enzyme-like activity, most researchers agree that the pro- and antioxidant properties of nanodispersed CeO_2 are

closely related to each other and are determined by several factors. According to the literature, the redox activity of nanodispersed cerium dioxide is influenced by the size and the shape of the particles, pH of the reaction medium, the presence of surface ligands, etc. Thus, in a recent study, a strong structure-sensitive peroxidase-mimetic activity of CeO_2 nanoparticles (nanocubes and nanorods) was revealed [40]. Two types of oxidants were identified in CeO_2/H_2O_2 systems: HO· and peroxidase-like intermediates, the formation of which strongly depends on pH and morphology of CeO_2 nanocrystals. The nature of the peroxidase-like activity of nanocrystalline cerium dioxide is mainly explained by formation of HO radicals under acidic conditions, while peroxide-like intermediates play an important role along with HO at neutral and basic pH values. In comparison with CeO_2 nanocubes, nanorods demonstrated higher peroxidase activity, due to the higher Ce^{3+} concentration and the concentration of oxygen vacancies [40].

Another factor influencing the redox activity of CeO_2 nanoparticles is surface functionalization. The prospects for biomedical applications of nanodispersed cerium dioxide necessitate the use of biocompatible ligands.

The effect of the stabilizer on the prooxidant potential of CeO_2 nanoparticles towards hydrogen peroxide in the presence of luminol was further analyzed. Kinetic curves and dependences of the analytical signal on the concentration were obtained for both non-stabilized CeO_2 nanoparticles and nanoparticles stabilized with ammonium citrate or maltodextrin (Fig. 6a,b).

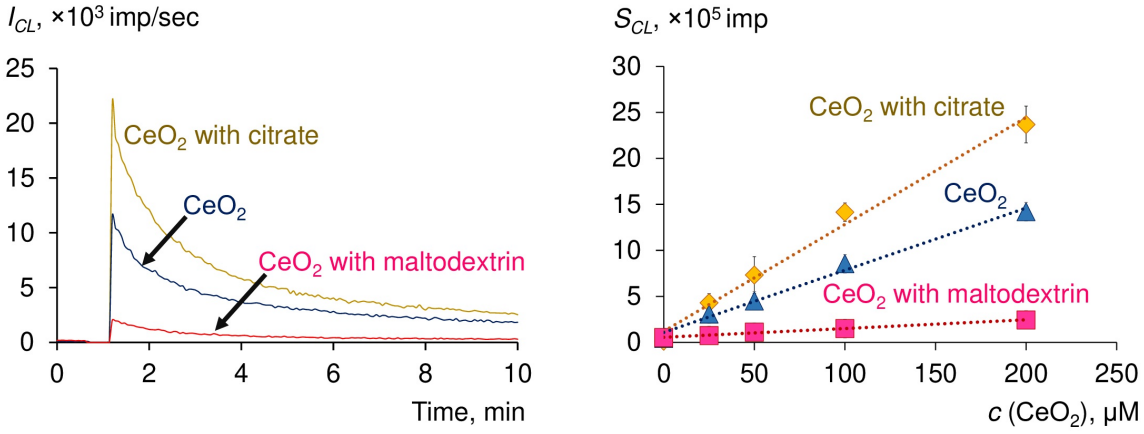

FIG. 6. Chemiluminescence of the luminol–H_2O_2 system in 100 μM PBS (pH 8.5) upon the addition of 200 μM non-stabilized colloidal solution of CeO_2 nanoparticles, citrate-stabilized CeO_2 sol or CeO_2 sol stabilized with maltodextrin in 100 μM PBS (pH 8.6) (a), the dependence of the light sum (S_{CL}, $\times$ 10^5 imp) on the concentration of CeO_2 sols (b). Conditions: 50 μM luminol, 200 μM H_2O_2, CeO_2 sols (concentrations are shown in the figure)

It can be seen that citrate-stabilized CeO_2 sol has the most pronounced prooxidant activity in comparison with the non-stabilized sol and maltodextrin-stabilized sol. Taking the prooxidant capacity of non-stabilized CeO_2 sol (200 μM) as 1, it follows that functionalization of the surface with ammonium citrate increases prooxidant capacity by two-fold, while maltodextrin decreases it by 6-fold. These results are consistent with previously published data on the protective effect of maltodextrin-stabilized CeO_2 nanoparticles against H_2O_2 [41]. Maltodextrin is considered the most promising non-toxic non-ionic stabilizer. The use of such stabilizers in the synthesis of therapeutic nanoparticles makes it possible to purposefully regulate their size and, accordingly, the ratio of pro- and antioxidant properties. Importantly, the polymer stabilizer does not prevent cerium dioxide particles from participating in redox processes and performing enzymatic functions.

Finally, the prooxidant capacity of the citrate-stabilized CeO_2 sol was estimated in the presence of phosphate species at pH 7.4, under physiologically relevant conditions. It is known that phosphate ions inhibit the biochemical activity of cerium dioxide by being adsorbed on the surface of nanoparticles [42, 43]. Chemiluminograms, as well as the dependence of the number of formed radicals on the concentration of CeO_2 citrate sol in Tris-HCl medium and phosphate buffer solutions are shown in Fig. 7a,b.

It was found that the prooxidant capacity of the citrate-stabilized CeO_2 sol in Tris-HCl buffer exceeds that for the case of a phosphate buffer by four-fold, which agrees well with the literature data on a decrease in the biochemical activity of nanodispersed cerium dioxide in the presence of phosphates [42, 43].

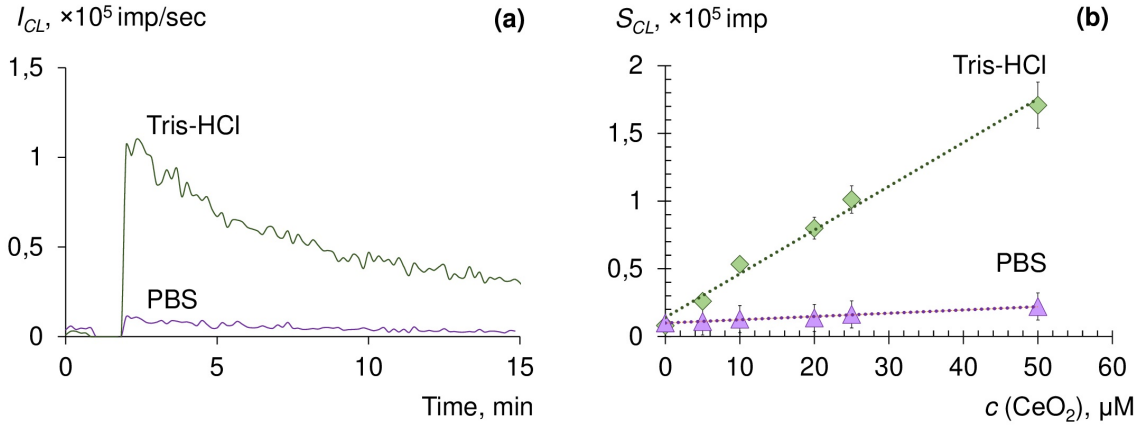

FIG. 7. Chemiluminograms for the luminol–H_2O_2 system in 100 μM Tris-HCl and PBS (pH 7.4) (are shown in the figure) upon the addition of the citrate-stabilized CeO_2 sol (a), the dependence of the light sum (S_{CL}, $\times$ 10^5 imp) on the citrate-stabilized CeO_2 sol (b). Conditions: 50 μM luminol, 200 μM H_2O_2, 200 μM the citrate-stabilized CeO_2 sol

5. Conclusion

A certain level of free radicals is constantly maintained in the body, which is necessary for normal life. Violations of the free radical balance inevitably lead to the development of diseases and pathological conditions. Special attention is currently paid to the search for drugs capable of regulating redox homeostasis. In this respect, CeO_2 nanoparticles are of particular interest, due to their multifaceted nanozyme activities, which makes it necessary to analyze the redox behavior of nanodispersed cerium dioxide with respect to key molecules involved in free radical reactions in the body.

In this work, to analyze the redox activity of CeO_2 nanoparticles, we used an approach that makes it possible to comprehensively assess their prooxidant potential towards hydrogen peroxide. Determination of the prooxidant capacity and prooxidant activity allows one not only to obtain quantitative characteristics for a comparative analysis of the enzyme-like activity of CeO_2 nanoparticles, but would allow further clarification of the mechanisms underlying this activity.

Acknowledgements

This work was supported by a grant from the President of the Russian Federation (project MK-2763.2021.1.3).

References

[1] Korsvik C., Patil S., et al. Superoxide dismutase mimetic properties exhibited by vacancy engineered ceria nanoparticles. *Chem. Commun. (Camb.)*, 2007, **10**, P. 1056–1058.

[2] Asati A., Santra S., et al. Oxidase-like activity of polymer-coated cerium oxide nanoparticles. *Angew. Chem. Int. Ed. Engl.*, 2009, **48**(13), P. 2308–2312.

[3] Pirmohamed T., Dowding J.M., et al. Nanoceria exhibit redox state-dependent catalase mimetic activity. *Chem. Commun. (Camb.)*, 2010, **46**(16), P. 2736–2738.

[4] Tian Z., Yao T., et al. Photolyase-Like Catalytic Behavior of CeO_2. *Nano Lett.*, 2019, **19**(11), P. 8270–8277.

[5] Xu F., Lu Q., et al. Nanoceria as a DNase I mimicking nanozyme. *Chem. Commun. (Camb.)*, 2019, **55**(88), P. 13215–13218.

[6] Yao T., Tian Z., et al. Phosphatase-like Activity of Porous Nanorods of CeO_2 for the Highly Stabilized Dephosphorylation under Interferences. *ACS Appl. Mater. Interfaces*, 2019, **11**(1), P. 195–201.

[7] Krysanov E.Y., Demidova T.B., et al. Synergetic action of ceria nanoparticles and doxorubicin on the early development of two fish species, *Danio rerio* and *Puntius tetrazona*. *Nanosystems: Phys. Chem. Math.*, 2019, **10**(3), P. 289–302.

[8] Thakur N., Prasenjit M., Das J. Synthesis and biomedical applications of nanoceria, a redox active nanoparticle. *J. Nanobiotechnol.*, 2019, **17**(1), P. 1–27.

[9] Hosseini M., Mozafari M. Cerium Oxide Nanoparticles: Recent Advances in Tissue Engineering. *Materials (Basel)*, 2020, **13**(14).

[10] Nyoka M., Choonara Y.E., et al. Synthesis of Cerium Oxide Nanoparticles Using Various Methods: Implications for Biomedical Applications. *Nanomaterials (Basel)*, 2020. **10**(2).

[11] Popova N.R., Andreeva V.V., et al. Fabrication of CeO_2 nanoparticles embedded in polysaccharide hydrogel and their application in skin wound healing. *Nanosystems: Phys. Chem. Math.*, 2020, **11**(1), P. 99–109.

[12] Rojkind M., Dominguez-Rosales J.A., et al. Role of hydrogen peroxide and oxidative stress in healing responses. *Cell. Mol. Life Sci.*, 2002, **59**(11), P. 1872–1891.

[13] Sozarukova M.M., Shestakova M.A., et al. Quantification of free radical scavenging properties and SOD-like activity of cerium dioxide nanoparticles in biochemical models. *Russ. J. Inorg.*, 2020, **65**, P. 597–605.

[14] Sozarukova M.M., Proskurnina E.V., et al. CeO_2 nanoparticles as free radical regulators in biological systems. *Nanosystems: Phys. Chem. Math.*, 2020, **11**(3), P. 324–332.
[15] Stone J.R., Yang S. Hydrogen peroxide: a signaling messenger. *Antioxid. Redox. Signal.*, 2006, **8**(3–4), P. 243–270.
[16] Sies H. Hydrogen peroxide as a central redox signaling molecule in physiological oxidative stress: Oxidative eustress. *Redox. Biol.*, 2017, **11**, P. 613–619.
[17] Geiszt M. Leto T.L. The Nox family of NAD(P)H oxidases: host defense and beyond. *J. Biol. Chem.*, 2004, **279**(50), P. 51715–51718.
[18] Li J., Stouffs M., et al. The NADPH oxidase NOX4 drives cardiac differentiation: Role in regulating cardiac transcription factors and MAP kinase activation. *Mol. Biol. Cell*, 2006, **17**(9), P. 3978–3988.
[19] Ushio-Fukai M. Localizing NADPH oxidase-derived ROS. *Sci. STKE*, 2006, **2006**(349), re8.
[20] Cai H. Hydrogen peroxide regulation of endothelial function: origins, mechanisms, and consequences. *Cardiovasc. Res.*, 2005, **68**(1), P. 26–36.
[21] Shcherbakov A.B., Teplonogova M.A., et al. Facile method for fabrication of surfactant-free concentrated CeO_2 sols. *Mater. Res. Express*, 2017, **4**(5), P. 055008.
[22] Jiao X., Song H., et al. Well-redispersed ceria nanoparticles: promising peroxidase mimetics for H_2O_2 and glucose detection. *Anal. Methods*, 2012, **4**(10), P. 3261–3267.
[23] White E.H., Zafiriou O., et al. Chemilunimescence of luminol: The chemcial reaction. *J. Am. Chem. Soc.*, 1964, **86**(5), P. 940–941.
[24] Merényi G., Lind J., Eriksen T.E. Luminol chemiluminescence: chemistry, excitation, emitter. *J. Biolumin. Chemilumin.*, 1990, **5**(1), P. 53–56.
[25] Khan P., Idrees D., et al. Luminol-based chemiluminescent signals: clinical and non-clinical application and future uses. *Appl. Biochem. Biotechnol.*, 2014, **173**(2), P. 333–355.
[26] Krasowska A., Rosiak D., et al. The antioxidant activity of BHT and new phenolic compounds PYA and PPA measured by chemiluminescence. *Cell. Mol. Biol. Lett.*, 2001, **6**(1), P. 71–82.
[27] Vladimirov Y.A., Proskurnina E.V. Free radicals and cell chemiluminescence. *Biochem. (Mosc.)*, 2009, **74**(13), P. 1545–1566.
[28] Li X., Zhang Z., et al. A chemiluminescence microarray based on catalysis by CeO_2 nanoparticles and its application to determine the rate of removal of hydrogen peroxide by human erythrocytes. *Appl. Biochem. Biotechnol.*, 2013, **171**(1), P. 63–71.
[29] Izmailov D.Y., Proskurnina E.V., et al. The effect of antioxidants on the formation of free radicals and primary products of the peroxidase reaction. *Biophysics*, 2017, **62**(4), P. 557–564.
[30] Zhang Z.F., Cui H., et al. Gold nanoparticle-catalyzed luminol chemiluminescence and its analytical applications. *Anal. Chem.*, 2005, **77**(10), P. 3324–3329.
[31] Li X., Sun Li, et al. Enhanced chemiluminescence detection of thrombin based on cerium oxide nanoparticles. *Chem. Commun*., 2011, **47**(3), P. 947–949.
[32] Xu S., Chen F., et al. Luminol chemiluminescence enhanced by copper nanoclusters and its analytical application. *RSC Adv.*, 2014, **4**(30), P. 15664–15670.
[33] Wang R., Yue N., Fan A. Nanomaterial-enhanced chemiluminescence reactions and their applications. *Analyst*, 2020, **145**(23), P. 7488–7510.
[34] Guo J.-Z., Cui H., et al. Ag nanoparticle-catalyzed chemiluminescent reaction between luminol and hydrogen peroxide. *J. Photochem. Photobiol.*, 2008, **193**(2–3), P. 89–96.
[35] Chen W., Hong L., et al. Enhanced chemiluminescence of the luminol-hydrogen peroxide system by colloidal cupric oxide nanoparticles as peroxidase mimic. *Talanta*, 2012, **99**, P. 643–648.
[36] Lousada C.M., Yang M., et al. Catalytic decomposition of hydrogen peroxide on transition metal and lanthanide oxides. *J Mol. Catal. A-Chem.*, 2013, **379**, P. 178–184.
[37] Liu Q., Ding Y., et al. Enhanced peroxidase-like activity of porphyrin functionalized ceria nanorods for sensitive and selective colorimetric detection of glucose. *Mater. Sci. Eng. C*, 2016, **59**, P. 445–453.
[38] Alizadeh N., Salimi A., et al. Intrinsic Enzyme-like Activities of Cerium Oxide Nanocomposite and Its Application for Extracellular H_2O_2 Detection Using an Electrochemical Microfluidic Device. *ACS Omega*, 2020, **5**(21), P. 11883–11894.
[39] Grulke E., Reed K., et al. Nanoceria: factors affecting its pro-and anti-oxidant properties. *Environ. Sci. Nano*, 2014, **1**(5), P. 429–444.
[40] Wei X., Li X., et al. Morphology-and pH-dependent peroxidase mimetic activity of nanoceria. *RSC Adv.*, 2018, **8**(21), P. 11764–11770.
[41] Shcherbakov A.B., Zholobak N.M., et al. Synthesis and antioxidant activity of biocompatible maltodextrin-stabilized aqueous sols of nanocrystalline ceria. *Russ. J. Inorg.*, 2012, **57**(11), P. 1411–1418.
[42] Singh S., Dosani T., et al. A phosphate-dependent shift in redox stateof cerium oxide nanoparticles and its effects on catalytic properties. *Biomaterials*, 2011, **32**(28), P. 6745–6753.
[43] Singh R., Singh S. Role of phosphate on stability and catalase mimetic activity of cerium oxide nanoparticles. *Colloids Surf. B: Biointerfaces*, 2015, **132**, P. 78–84.